

# Probabilistic Safety Assessment of Concrete Columns by Approximate Bayesian Computation

Manuel Chiachío Ruano

*Structural Mechanics and Hydraulics Engineering Department, University of Granada, Spain.*  
E-mail: [mchiachio@ugr.es](mailto:mchiachio@ugr.es)

José Barros Cabezas

*Civil Engineering Faculty, Catholic University of Santiago de Guayaquil, Ecuador.*  
E-mail: [jose.barros@cu.ucsg.edu.ec](mailto:jose.barros@cu.ucsg.edu.ec)

Juan Chiachío Ruano

*Structural Mechanics and Hydraulics Engineering Department, University of Granada, Spain.*  
E-mail: [jchiachio@ugr.es](mailto:jchiachio@ugr.es)

Engineering practice commonly requires the calibration of complex numerical models based on experimental data, which is typically carried-out as a trial and error process whose success is highly influenced by human errors. The Bayesian procedure is a robust methodology to solve this problem which also allows quantification of the uncertainties. However, this procedure requires the knowledge of a likelihood function, which sometimes is difficult to evaluate or directly impossible to obtain. For such cases, the Approximate Bayesian Computation (ABC) method is an efficient alternative to address the calibration of a complex numerical probabilistic model based on data. This paper presents the applicability of the ABC method using an efficient algorithm called ABC-SubSim for the calibration of a complex non-linear mechanical model. A set of uncertain model parameters from a reinforced concrete column subjected to lateral cyclic loads, are indirectly inferred with quantified uncertainty with a low computational cost. These parameters are difficult to observe experimentally and are crucial to assess the structural vulnerability and safety under seismic loads. Results show that the proposed methodology reduces the uncertainty about the mechanical parameters and makes them learn from the data, hence making this algorithm useful for uncertainty management and safety assessment. Influence of axial load on reinforced concrete beam-column models is also discussed. Finally, the paper discusses further improvements required for the ABC-SubSim based on sensitivity analysis and numerical trials carried-out over the course of this research.

*Keywords:* ABC-SubSim, concrete structures, seismic assessment, Bayesian inference

## 1. Introduction

Seismic performance evaluation methods are key assessment studies for evaluating the safety of existing structures under seismic events. Complex multi-dimensional, non-linear structural models are typically required for performing a seismic evaluation, however their model accuracy is highly dependent on complex calibrations of the model parameters based on previous test results (as the concrete model proposed in Haselton et al. (2008)). These procedures are usually carried out by trial and error methods that could lead to inaccurate estimations of performance. For example, in FEMA P695 (Harris et al., 2009), which is a document that proposes a methodology to determine seismic design factors from the results of series of non-linear time-history analyses, it is emphasized that the probability of collapse is

highly dependent of in-cycle degradation parameters. Several test results are required to correctly validate the degradation parameters, so an algorithm based solution should be taken in order to minimize the human factor error.

During the development of the aforementioned methodology, Ibarra et al. (2005) proposed a numerical model of non-linear response capable of considering, explicitly and efficiently, the different types of degradation. This model, known as *IMK* model, was further used by Haselton et al. (2008) to develop a series of regression equations to estimate the parameters that allows the evaluation of the moment-rotation behaviour of a reinforced concrete beam-column. As trial and error procedure was used, over-adjustment to the data is expected, creating a lack of hardness outside the set of the data. Also, axial-flexural interaction was neglected leading to lower than

expected deformation estimates.

In order to address this problem, the Bayesian inverse inference methodology could be useful for the calibration of a complex model as it allows: (a) considering the uncertainty of the parameters, models and data, (b) quantify and reduce the uncertainties based on information proposed by data, (c) obtain the *a posteriori* information of the parameters, that indicates a range of values of these parameters in terms of the experimental data.

From available Bayesian methods, Approximated Bayesian Computation methodology (Marjoram et al., 2003) (ABC) is proposed in this investigation because of its versatility in cases where likelihood function may be hard to compute, or directly unknown. ABC replaces the likelihood with a computational evaluation of the model (with the mentioned uncertainties). The application of the approximate Bayesian methods has been used in the inference of numerical models in other sciences, such as molecular dynamics (Kulakova, 2017). Other authors as Song et al. (2019) and Zuev et al. (2012) propose the use of the approximate Bayesian methods to structural dynamic and non-linear models, respectively, with positive results.

In this paper, an example of the calibration of a complex numerical model is carried out using the ABC-SubSim algorithm (Approximate Bayesian Computation by Subset Simulation) originally proposed in Chiachio et al. (2014). General characteristics of the algorithm are also presented. An axial-flexural interaction model is calibrated from a test done by others (Gill, 1979). Finally, the calibrated model is used for the estimation of the lateral deformation of a single story reinforced concrete frame subjected to a seismic acceleration. Results are compared to a model with flexural elements without axial load interaction.

## 2. Approximate Bayesian Computation by Subset Simulation (ABC-SubSim) Algorithm

The ABC-SubSim algorithm, originally presented in Chiachio et al. (2014) for model-based parameter identification, is an approximate Bayesian computation algorithm capable to produce precise posterior information of model parameters without the need of a likelihood function. In this work, the ABC-SubSim method is used to estimate nonlinear model parameters based on real-life structural tests results. Synoptically, the process followed by the algorithm includes the following steps (also shown in Algorithm 1):

- Given a numerical model  $F(\theta)$  based on a set of updatable model parameters  $\theta = \{\theta_1, \theta_2, \dots, \theta_n\} \in \mathbf{R}^{n_\theta}$ , define an objective function  $f(\theta) : \mathbf{R}^{n_\theta} \rightarrow \mathbf{R}$  such that:

---

### Algorithm 1 ABC-SubSim

---

**Require:**  $p_0 \in [0, 1]$  {defines the number of seeds by  $Np_0$  and the number of Markov Chains for each subset by  $\frac{1}{p_0}$ };  
 $N$ , {number of samples per intermediate level};  
 $\epsilon_f, m$ , {final tolerance value and maximum number of Subsets, for breaking criteria};  
Objective Function:  $\epsilon = f(\theta_1, \theta_2, \dots, \theta_{n_p})$

**Ensure:**  $\theta_1, \theta_2, \dots, \theta_{n_p}$   
*Monte-Carlo Simulations*  
1: Sample  $[\theta_{1,i}^{(0)}, \dots, \theta_{1,i}^{(n)}, \dots, \theta_{1,i}^{(N)}]$  for  $i = 1, \dots, n_p$   
2: **for**  $n = 1, \dots, N$  **do**  
3: Evaluate tolerance function:  $\epsilon_1^{(n)} = f(\theta_{1,1}^{(n)}, \theta_{1,2}^{(n)}, \dots, \theta_{1,n_p}^{(n)})$   
4: **end for**  
*Subset Simulation*  
5: **for**  $j = 2, \dots, m$  **do**  
6: Renumber  $[\theta_{j-1,i}^{(n)}, n : 1, \dots, N, i = 1, \dots, n_p]$   
so that  $\epsilon_{j-1}^{(1)} \leq \epsilon_{j-1}^{(2)} \leq \dots \leq \epsilon_{j-1}^{(N)}$   
7: **for**  $k = 1, \dots, Np_0$  **do**  
8: Select  $(\theta_{j-1,i}^{(k)})$  as a seed  
*Markov-Chain Monte-Carlo*  
9: **for**  $l = 1, \dots, \frac{1}{p_0}$  **do**  
10: Generate child conditional samples  $\theta_{j,i}^{k,l}$   
from the seed  $\theta_{j-1,i}^{(k)}$   
11: Evaluate tolerance function  $\epsilon_l$   
12: **if**  $\epsilon_l \leq \epsilon_{j-1}^{(Np_0)}$  **then**  
13: Accept the child sample  $\theta_{j,i}^{k,l}$  as new sample  
14: **else**  
15: Use seed  $\theta_{j-1,i}^{(k)}$  as new sample  
16: **end if**  
17: **end for**  
18: Reorder  $[\theta_{j,i}^{(k),l} : k = 1, \dots, Np_0; l = 1, \dots, \frac{1}{p_0}]$  as  $[\theta_{j,i}^{(1)}, \dots, \theta_{j,i}^{(N)}]$   
19: **end for**  
20: **if**  $\epsilon_j^{(Np_0)} \leq \epsilon_f$  **then**  
21: End algorithm  
22: **end if**  
23: **end for**

---

$$f_{obj} = \min \left( \sum |F^* - F(\theta)| \right) \quad (1)$$

- where  $F^*$  is the measured data during the test;
- Define a Monte Carlo analysis using  $N$  parameter samples  $\theta^{(1)}, \theta^{(2)}, \dots, \theta^{(N)}$ , then evaluate and reorder the resulting set based on the objective function values following an ascending order;

- Produce Markov Chain samples to populate the parameter space from the  $(N p_0)$ 's first values (acting as *seeds* values) so that the remaining  $N(1 - p_0)$ 's values are produced according to the objective function values. The parameter  $p_0$  is a tuning parameter called *conditional probability* with suggested values ranging in the interval  $[0.1, 0.3]$  Chiachio et al. (2014);
- The previous step produces a new *subset* of size  $N$ . After producing each *subset*, the parameter values are reordered based on the basis of the objective function values, hence the sampling procedure (Markov Chain) is repeated again until a tolerance value  $\epsilon$  is obtained or until a maximum number of subsets (previously defined) are reached.

As a result, a multi-dimensional posterior distribution about the model parameter  $\theta$  is obtained. This posterior distribution gives information about the plausibility of the values of  $\theta$  that better reproduce the model response based on the structural data set.

### 3. Structural nonlinear model

This section presents the nonlinear mechanical model used for the seismic assessment. The model reproduces the response of a reinforced concrete column with applied constant axial load and subjected to cyclic lateral deformation. The details of the nonlinear model of the reinforced concrete beam-column are presented in section 3.1. Specific model information about a case-study test performed by Gill (1979) on the reinforced concrete beam-column, is presented in section 3.2.

#### 3.1. Characteristics of the non-linear model of a reinforced concrete column

The structural model is conceived as a cantilever column modelled as a non-linear *force-based beam-column* element with a rotational spring in its boundary, as shown in Figure 1. The numerical implementation is carried out in OpenSeespy (Zhu et al., 2018) library on Python software. The reinforced concrete section is represented by a *fiber* section, where the cross-section is discretised in a series of elements with uniaxial behaviour, such that the axial-flexural stiffness of the section is determined by integration of the stiffness of the uniaxial elements over the section. Concrete behaviour is represented by the *Concrete01* constitutive model (see Figure 2), using as inputs the recommendations proposed in Karthik and Mander (2011) and the estimation of the confinement ratio proposed in Mander et al. (1988). The steel reinforcement behaviour was modelled with the *Hysteretic* constitutive model (see Figure 3) and the recommended properties of the ASCE/COPRI

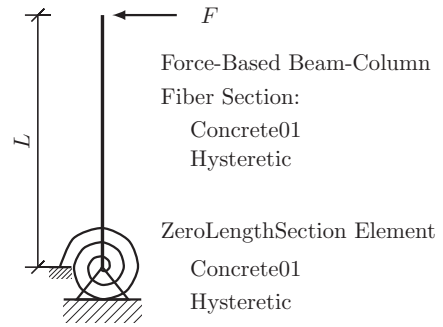


Fig. 1. Nonlinear structural model of a reinforced concrete beam-column in OpenSeespy.

(2014) regulations. All the materials constitutive's values were defined with the nominal resistance reported by Gill (1979). Note also that the *Hysteretic* model allows considering resistance and stiffness deterioration by three parameters: (1) demanded ductility of the material (named as  $dmg_1$ ), (2) dissipated energy (called  $dmg_2$ ), and (3) by the pinching parameter (called  $\beta$ ). Through these three parameters, the degradation of a reinforced concrete beam-column element can be modelled, which is a critical requirement for the seismic performance evaluation of a structure (Harris et al. (2009), Haselton et al. (2008)).

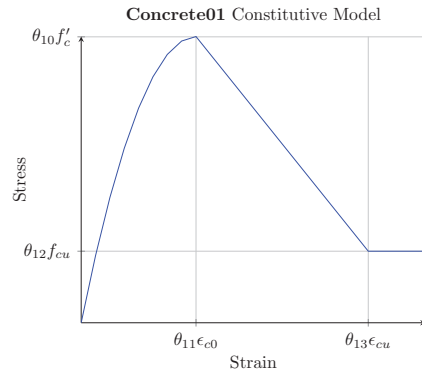


Fig. 2. *Concrete01* material constitutive model and calibration parameters.

#### 3.2. Case study

A 3300 [mm] length  $550 \times 550$  [mm<sup>2</sup>] cross-section column is considered in this case study. The longitudinal reinforcement ratio is equal to 0.0179 considering a 40 [mm] clear cover Gill (1979); Berry et al. (2004), thus resulting an average compressive strength of the concrete of 23.1 [MPa]. On the other hand, the yield strength of

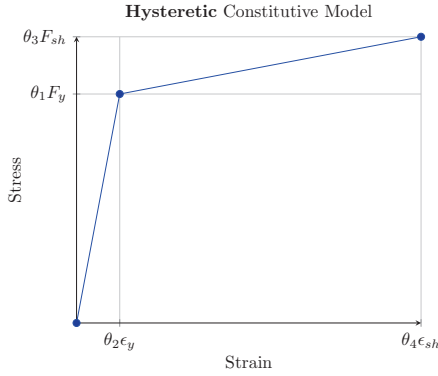


Fig. 3. Hysteretic material constitutive model and calibration parameters.

longitudinal reinforcement is 375 [MPa] whilst the yield strength of transverse reinforcement is 297 [MPa], with transverse reinforcement of 10 [mm] diameter, spaced every 80 [mm] in the critical area.

Figure 4 shows the schematic diagram of the test, indicating that the specimen was axially loaded with a constant compressive load of 1815 [KN] and also subjected to cyclic displacements varying from  $\pm 5$  [mm] to  $\pm 35$  [mm] applied to the mid span. Figure 5 shows the force and lateral displacement results.

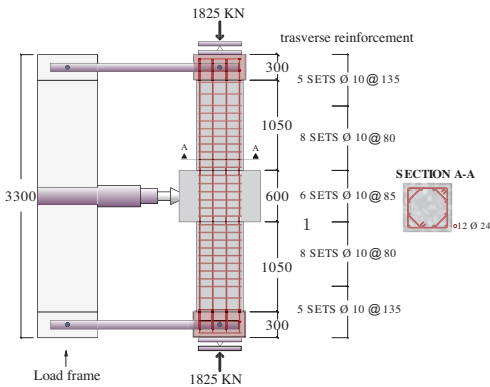


Fig. 4. Set-up configuration from the Gill (1979) test.

#### 4. Results and Discussion

The ABC-SubSim algorithm is applied to infer the mechanical parameters of the non-linear structural performance model, using  $N = 2000$  samples and  $p_0 = 0.2$ . Although  $p_0$  parameter selection will not influence the final results, it is important for the efficiency of the algorithm. Several trials were needed in order to define this particular parameter. The maximum amount of *Subsets* was limited to

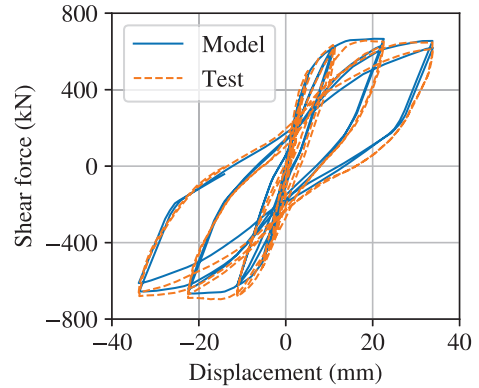


Fig. 5. Comparison between test and calibrated model force-displacement results.

$m = 20$ , with a tolerance value  $\epsilon$  equal to:

$$\epsilon_f = 0.10 \sum_{i=1}^{N^*} (F^*)_i \quad (2)$$

where  $N^*$  is the number of data points of the test results.

Thirteen updatable model parameters have been selected for the model calibration, i.e.  $\theta = \{\theta_1, \theta_2, \dots, \theta_{13}\}$ . The parameters  $\theta_1$  to  $\theta_4$  correspond to coefficients of resistance and deformation of steel reinforcement constitutive values, as shown in Figure 3. Parameters  $\theta_5$  and  $\theta_6$  are to define the pinching of the response of the steel reinforcement model. Next,  $\theta_7$  to  $\theta_9$  are degradation parameters of the hysteretic model corresponding to  $dmg_1$ ,  $dmg_2$  and  $\beta$ , respectively. Finally, parameters  $\theta_{10}$  to  $\theta_{13}$  correspond to coefficients of the resistance and deformation values for the concrete constitutive behaviour, as shown in Figure 2.

Figure 5 shows the comparison of the cyclic response of the column from the test and using the inferred model after applying the ABC-SubSim algorithm. As can be observed, the model response agrees reasonably well to the test data in terms of strength and deformation. Figure 6 gives the objective function values per simulation level showing that it gets minimized as the algorithm progress. For this example, after subset number 15, the error reached almost a constant value meaning that the corresponding  $\theta$  optimum values have already been reached at subset 15.

Moreover, Figure 7 presents a multidimensional scatter-plot of the posterior samples of  $\theta_1$  to  $\theta_6$ , chosen for illustration purposes. A colour code of increasing intensity is used to differentiate between subsets, corresponding the darker colors to the latest (15<sup>th</sup> subset). The diagonal shows the probability density functions (PDFs) of each parameter, whilst the rest of the plots show paired

Table 1. Parameter a priori information and posteriori results.

		$\theta_1$	$\theta_2$	$\theta_3$	$\theta_4$	$\theta_5$	$\theta_6$	$\theta_7$	$\theta_8$	$\theta_9$	$\theta_{10}$	$\theta_{11}$	$\theta_{12}$	$\theta_{13}$
A Priori	Lower Bound	0.50	0.50	0.50	0.50	0.00	0.50	0.00	0.00	0.00	0.50	0.50	0.50	0.50
	Upper Bound	1.50	1.50	1.50	1.50	0.50	1.00	0.25	0.25	0.25	1.50	1.50	1.50	1.50
Maximum a Posteriori (MAP)		1.11	1.07	1.20	1.02	0.50	0.70	0.011	0.212	0.189	0.73	1.34	0.93	0.57
Standard Deviation (%)		0.73	1.27	0.64	3.00	0.56	0.84	0.03	1.07	0.46	0.28	0.70	1.14	0.98

scatter dispersion plots for every pair of parameters. Note that the uncertainty of all parameters (which can be noticed by considering the spread of each PDF) is significantly reduced as they are confronted with experimental data. Also, the uncertainty is reduced as the algorithm progress towards deeper subsets meaning that there is an effective model learning from the data. Table 1 summarizes the values of each model parameter at the beginning (by the a priori parameter range) and end of the process (by the maximum a posteriori [MAP]). This results show that the resulting model using the MAP values as model parameters is the most suitable one to reproduce the test data.

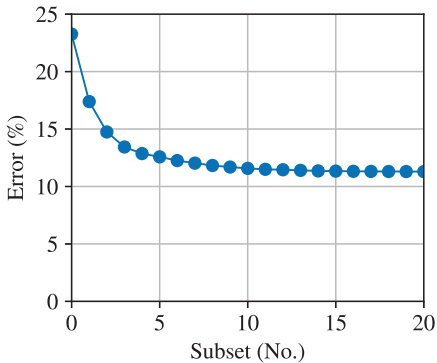


Fig. 6. Evolution of model error during calibration process.

It can be noticed that the uncertainty reduction of parameter  $\theta_4$ , which corresponds to the coefficient of the nominal ultimate deformation of the steel reinforcement, is significantly less than the others. Indeed, the standard deviation values of the posterior PDFs taken from table 1 corroborate this appreciation, showing the highest standard deviation value for  $\theta_4$ . This means that this parameter is relatively insensitive to the information provided by data and, therefore, its variation has less effect on the force-deformation response of the tested element. This result is consistent with the physical condition of the test, as this parameter modifies the ultimate deformation capacity of the

steel reinforcement, which corresponds to a deformation level not reached during the test.

Finally, the calibrated model is used for a non-linear dynamic analysis of an one-bay and one-story reinforced concrete frame, as shown in Figure 8. The columns are modelled with the MAP parameter results and the beam is modelled as a linear-elastic element with the same geometric properties as the columns and a Young Modulus equal to  $22.5\text{ GPa}$ . A second model using *IMK* constitutive model from Ibarra et al. (2005) and parameters from Haselton et al. (2008) was also constructed for comparative purposes (see Figure 8). For both models, the following considerations were adopted: (1) roof mass equal to  $455\text{ kg}$ , (2) 5% of critical damping using Rayleigh mass and stiffness proportional formulation and, (3) Chichi, Taiwan 1999 seismic acceleration N-S record from CHY101 seismic station was used as lateral load.

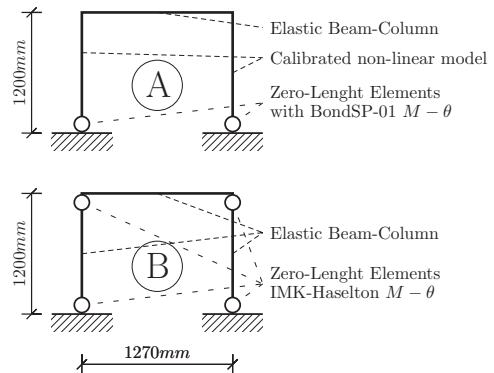


Fig. 8. One-bay and one-story frame models. "A" model was constructed based on calibrated non-linear beam-column model presented in this investigation. "B" model is constructed based on IMK-Haselton model.

Figure 9 displays the lateral deformation, first column axial and shear force results for both models. As can be seen, similar results are obtained

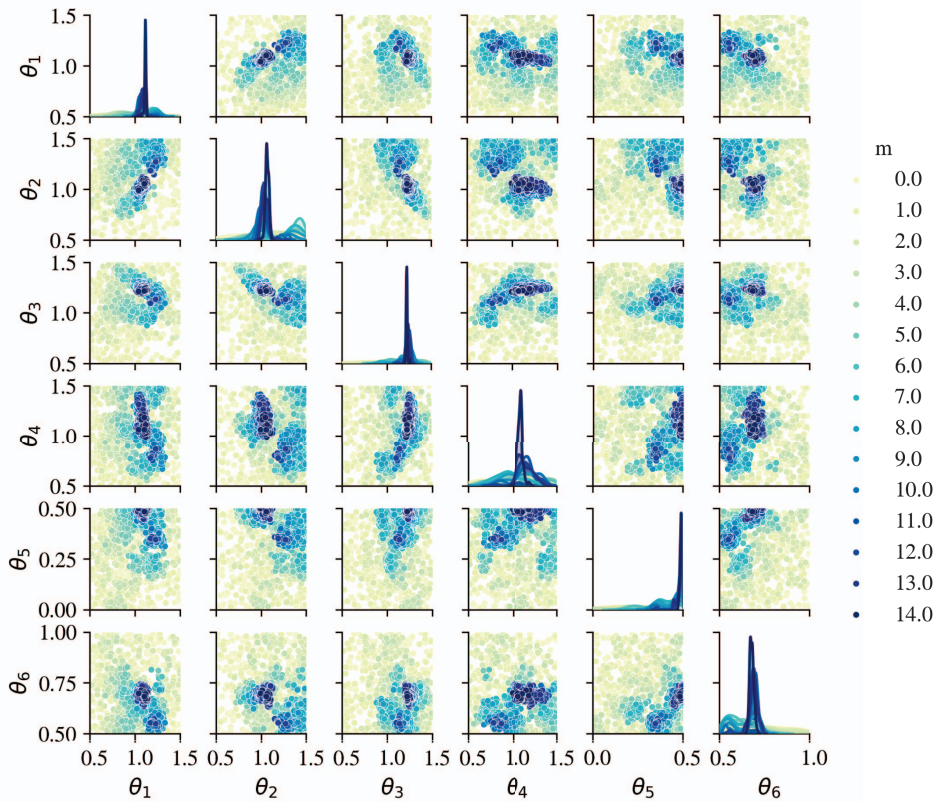


Fig. 7. Scatter plot matrix results for  $\theta_1$  to  $\theta_6$  parameters. Axes in the diagonal display the density plots of the corresponding parameter (only 6 parameters and the initial 14 subsets are presented for clarity).

until the 35th second of the history, where higher deformations are attained by A-model, leading to higher shear and axial forces. As expected, maximum axial and shear forces resulted very similar for both models, as they have similar resistance; however, lateral deformations displayed significant difference, as A-model stiffness updates for each step according to both axial load variations and deformation levels, and B-model only updates for the latter.

Table 2 compares the maximum deformations resulted for both models when subjected to different gravitational loads, showing significant axial load influence on estimated lateral deformation.

### 5. Conclusion

In order to perform a probabilistic safety assessment of concrete columns, complex non-linear model calibration is required. In this article, model parameters were inferred using the approximate Bayesian computation by Subset Simulation algorithm, including the quantification of the model uncertainty for each parameter, based on real test results. From the presented analyses, the

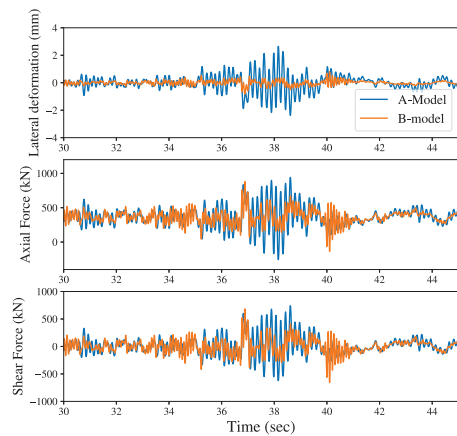


Fig. 9. Non-linear time history analysis results: (1) Lateral deformation, (2) axial force at first column and (3) shear force at first column.

Table 2. Axial load influence on calculated lateral deformation.

Axial Load (kN)	Absolute Maximum $\delta_{roof}$ (mm)	
	A-model	B-model
1800.0	1.5	0.8
900.0	1.6	0.8
180.0	2.8	0.8

following conclusions can be drawn:

- The PDF of each parameter gives additional information about how they help to explain the data. Less important parameters will have larger deviations. This also have good agreement with expected behaviour of the real test, as shown in section 4.
- The axial-flexural interaction of reinforced concrete columns should be taken into account for non-linear dynamic modelling; care must be taken when using only-flexural elements as they are unable to update the stiffness from the variable axial loads.

Future work will include a study of the  $p_0$  parameter selection to maximize the efficiency of the algorithm and the calibration of the model for a series of concrete column tests in order to propose regression equations for the parameters.

### Acknowledgement

This work was supported by the SINDE (Sistema de Investigación y Desarrollo) of the UCSG (Universidad Católica de Santiago de Guayaquil), project Cod. Pres. #491 / Cod. Int. #170. The authors are grateful to Joel Consuegra and Frank Cabanilla for editing assistance during the elaboration of this paper.

### Citations and References

#### References

ASCE/COPRI (2014). *Seismic Design of Piers and Wharves*. ASCE/COPRI.

Berry, M., M. Parrish, and M. Eberhard (2004). *PEER Structural Performance Database User's Manual (Version 1.0)*. PEER.

Chiachio, M., J. L. Beck, J. Chiachio, and G. Rus (2014). Approximate bayesian computation by subset simulation. *SIAM Journal on Scientific Computing* 36(3), A1339–A1358.

Gill, W. (1979). *Ductility of rectangular Reinforced Concrete Columns with axial load*. Ph. D. thesis, University of Canterbury.

Harris, J. R., J. A. Heintz, P. Manager, J. Hooper, A. R. Porush, S. Cranford, K. Haas, and C. Haselton (2009). *Quantification of Building*

*Seismic Performance Factors*. Federal Emergency Management Agency.

Haselton, C. B., A. B. Liel, and S. T. Lange (2008). *Beam-Column Element Model Calibrated for Predicting Flexural Response Leading to Global Collapse of RC Frame Buildings*. PEER.

Ibarra, L. F., R. A. Medina, and H. Krawinkler (2005). Hysteretic models that incorporate strength and stiffness deterioration. *Earthquake Engineering and Structural Dynamics* 34(12), 1489–1511.

Karthik, M. M. and J. B. Mander (2011). Stress-block parameters for unconfined and confined concrete based on a unified stress-strain model. *Journal of Structural Engineering* 137(2), 270–273.

Kulakova, L. (2017). *Bayesian Uncertainty Quantification for Data-Driven Applications in Engineering and Life Sciences*. Ph. D. thesis, ETH Zurich.

Mander, J. B., N. Priestley, and R. Park (1988). Theoretical stress-strain model for confined concrete. *Journal of structural engineering* 114(8), 1804–1826.

Marjoram, P., J. Molitor, V. Plagnol, and S. Tavaré (2003). Markov chain monte carlo without likelihoods. *Proceedings of the National Academy of Sciences* 100(26), 15324–15328.

Song, M., I. Behmanesh, B. Moaveni, and C. Papadimitriou (2019). Modeling error estimation and response prediction of a 10-story building model through a hierarchical bayesian model updating framework. *Frontiers in Built Environment* 5(January), 1–15.

Zhu, M., F. McKenna, and M. H. Scott (2018). Openseespy: Python library for the opensees finite element framework. *SoftwareX* 7, 6–11.

Zuev, K. M., J. L. Beck, S. K. Au, and L. S. Katafygiotis (2012). Bayesian post-processor and other enhancements of subset simulation for estimating failure probabilities in high dimensions. *Computers and Structures* 92-93, 283–296.